Epithelial defect repair in the auricle and auditory meatus by grafting with cultured adipose-derived mesenchymal stem cell aggregate-extracellular matrix

Wen-Jin Zhang[1,2], Lei-Guo Ming[3,4], Jian-Jun Sun[1,2]

[1]Center of Otolaryngology Head and Neck Surgery, Chinese PLA Navy General Hospital, Beijing 100048, China;
[2]School of Postgraduate, Anhui Medical University, Hefei, Anhui 230032, China;
[3]State Key Laboratory of Military Stomatology, Center for Tissue Engineering, School of Stomatology, Fourth Military Medical University, Xi'an, Shaanxi 710032, China;
[4]Research and Development Center for Tissue Engineering, Fourth Military Medical University, Xi'an, Shaanxi 710032, China.

Abstract

Background: Several patients experience persistent otorrhea after a flawless surgical procedure because of insufficient epithelial healing. Several efforts, such as autologous tissue allograft and xenograft, have been made to halt otorrhea. However, a stable technology to induce temporal epithelial repair is yet to be established. Therefore, this study aims to investigate whether implantation of seeding adipose-derived mesenchymal stem cell (ADMSC) aggregates on extracellular matrix (ECM; herein, ADMSC aggregate-ECM) into damaged skin wound promotes skin regeneration.

Methods: ADMSC aggregate-ECM was prepared using a previously described procedure that isolated ADMSCs from rabbits and applied to the auricle and auditory meatus wound beds of New Zealand white rabbits. Wound healing was assessed by general observation and hematoxylin and eosin (H&E) staining. Secretion of growth factor of the tissue was evaluated by western blotting. Two other groups, namely, ECM and control, were used. Comparisons of three groups were conducted by one-way analysis of variance analysis.

Results: ADMSCs adhered tightly to the ECM and quickly formed cell sheets. At 2 weeks, general observation and H&E staining indicated that the wound healing rates in the ADMSC aggregate-ECM ($69.02 \pm 6.36\%$) and ECM ($59.32 \pm 4.10\%$) groups were higher than that in the control group ($43.74 \pm 12.15\%$; $P = 0.005$, $P < 0.001$, respectively) in ear auricle excisional wounds. At 7 weeks, The scar elevation index was evidently reduced in the ADMSC aggregate-ECM (2.08 ± 0.87) and ECM (2.31 ± 0.33) groups compared with the control group (4.06 ± 0.45; $P < 0.001$, $P < 0.001$, respectively). In addition, the scar elevation index of the ADMSC aggregate-ECM group reached the lowest rate 4 weeks in advance. In auditory meatus excisional wounds, the ADMSC aggregate-ECM group had the largest range of normal skin-like structure at 4 weeks. The ADMSC aggregate–ECM and ECM groups secreted increased amounts of growth factors that contributed to skin regeneration at weeks 1 and 2, respectively.

Conclusions: ADMSC aggregate-ECM and ECM are effective repair materials for wound healing, especially ADMSC aggregate-ECM. This approach will provide a meaningful experimental basis for mastoid epithelium repair in subsequent clinical trials.

Keywords: Adipose-derived mesenchymal stem cell; Extracellular matrix; Otorrhea; Rabbit; Skin regeneration; Wound healing

Introduction

Surgical removal is the treatment of choice for congenital and acquired concha atresia deformity, external auditory canal malignant tumor, and chronic suppurative attic-oantral disease in middle ear cleft. A frequently performed surgical procedure results in concha skin defects and exposure of the temporal bone mastoid cavity to the external bone surface. However, complete healing after surgery depends on the epidermal level of the wound. Delayed epithelialization can lead to long-term otorrhea, superinfection, and granulation formation, which further prevent epithelial healing and affect the quality of life of a patient. Clinical studies found that, in nearly one in three patients, epithelialization is absent or occurs sufficiently quick before the onset of infection.[1]

Efforts have been made to halt otorrhea and infection by obliterating the mastoid cavity with a thick skin graft,[2] a temporal muscle fascia-periosteum flap,[3] bone pate,[4]

Access this article online

Quick Response Code:

Website: www.cmj.org

DOI: 10.1097/CM9.0000000000000125

Wen-Jin Zhang and Lei-Guo Ming contribute equally to this paper.

Correspondence to: Prof. Jian-Jun Sun, Center of Otolaryngology Head and Neck Surgery, Chinese PLA Navy General Hospital, Beijing 100048, China
E-Mail: jjsun85@sina.com

Chinese Medical Journal 2019;132(6)

Received: 13-01-2019 **Edited by:** Li-Min Chen

and beta-tricalcium phosphate.[5] However, none of these techniques have achieved satisfactory results. Meanwhile, skin tissue engineering techniques, such as application of various cells, scaffolds, and growth factors, have been explored to accelerate skin regeneration. This approach, which is performed entirely on an out-patient basis without general anesthesia, has been extensively investigated to control otorrhea in several centers, where several cases obtained satisfactory effects.[1,6-9] However, this approach also presents major disadvantages. (1) A long waiting period (3–4 weeks) is required from the expansion of cells to harvesting of multilayer cell sheets. Moreover, (2) the brittle and thin cell sheets are difficult to operate when used to cover the wound area and entire wound. Furthermore, (3) the approach exhibits a low success rate after transplantation (4) and low vascularization, both of which limit the supply of immune cells, nutrients, and oxygen to the wound area.[10]

To solve these problems, we combined adipose-derived mesenchymal stem cell (ADMSC) sheets with extracellular matrix (ECM) scaffolds (herein, ADMSC aggregate-ECM) to treat full-thickness defects and test the effects of ADMSC aggregate-ECM in a rabbit skin injury model. ADMSCs have been shown to secrete various tissue-healing promoters and growth factors,[11,12] lack type-II major histocompatibility complex and cell surface stimulus molecule expression,[13] and exhibit the least immune response in an allogeneic host.[14] ADMSCs are isolated from a small volume of adipose tissue and expand easily *in vitro*,[14,15] which suggests the potential use for these cells in therapeutic tissue engineering. ECM scaffolds have been successfully used for wound repair in preclinical animal studies and human clinical applications.[16] They are harvested from the small intestine, skin, liver, pancreas, and urinary bladder, among other tissues. The preparation of ECM scaffolds requires several steps, such as decellularization, hydration, dehydration, and sterilization, to remove the resident cells and retain the integrity and ratios of the collagen structure in the natural dermal matrix. The developed matrices have been proven to exhibit vascularization capacities *in vivo*[15,17] Therefore, we hypothesized that the combination of ADMSCs and ECM scaffold not only serves as cell carriers that provide mechanical support but also facilitate cell-scaffold interactions, which actively influence cellular responses, such as proliferation, angiogenic growth factor secretion, and skin formation.

Methods

Ethical approval

The study was conducted in accordance with the *Declaration of Helsinki* and was approved the Animal use and Care Committee of the Fourth Military Medical University (License number: SCXK 2007-007).

Isolation and culture of ADMSCs

Two-week-old New Zealand white rabbits were provided by the Institute of Neuroscience of the Fourth Military Medical University. Adipose tissue was obtained from the inguinal region of the rabbits and extensively washed three times with phosphate-buffered saline (PBS) to remove the pelleted stromal vascular fraction. The separated fatty tissue was then digested with 0.3% (w/v) collagenase type I (Sigma-Aldrich, USA) and shaken at 37°C for 1 h. An equal volume of α-minimum essential medium (MEM; Gibco, USA) that was supplemented with 10% fetal bovine serum (FBS; Gibco, USA), 0.292 mg/mL glutamine, 100 units/mL penicillin, and 100 μg/mL streptomycin (all from Sigma-Aldrich, USA) was added in the digested tissue to neutralize collagenase. The solution was filtered through a 100 μm cell strainer to remove undigested tissue fragments, centrifuged at 1000 r/min for 10 min, and resuspended in 10 mL of α-MEM. This suspension was placed in T75 flasks and incubated at 37°C in a humidified chamber that contained 5% CO_2. After 3 days, non-adherent cells and debris were depleted by replacing the medium with a fresh medium. After reaching 80% to 90% confluence and changing the medium every 2 days, the cells were harvested with trypsin and sub-cultured.

Characterization of ADMSCs

Flow cytometry analysis

The phenotype of cultured ADMSCs was evaluated by flow cytometry. Cells at passage five were harvested by trypsin and resuspended in PBS. Approximately 1×10^6 cells were incubated with the following: fluorescein isothiocyanate-conjugated rabbit CD14 (Thermo, USA), CD90 (Abcam, UK), CD29 (Novus, USA), and CD45 (Santa Cruz, USA). In addition, phycoerythrin-goat anti-rabbit lgG (Novus, USA) and FITC-conjugated goat anti-mouse lgG (Santa Cruz, USA) secondary antibodies were used. Cells without incubated antibodies were used as controls. Subsequently, all cells were analyzed using the Elite ESP flow cytometry system (Beckman Coulter, USA).

Proliferation of ADMSCs

Proliferation of cells was quantified using the 3-(4, 5-dimethylthiazol-2-yl)-2, 5-diphenyltetrazolium bromide (MTT, Beyotime, China) assay. ADMSCs were seeded at a concentration of 4.7×10^3 cells/cm^2 in a 96-well plate. At 1 to 9 days, 200 μL of culture medium and 20 μL of MTT reagent (5 mg/mL) were added to every specimen. After incubation for 4 h in a CO_2 incubator, all liquid mixtures were carefully discarded, and 150 μL of dimethyl sulfoxide (Beyotime, China) was added to the 96-well plates. Next, the absorbance of each well was measured by a micro-plate reader at a wavelength of 490 nm after oscillation for 10 min. Background absorbance was corrected by subtracting the absorbance index of the culture medium from the specimen data.

Adipogenic differentiation assays

A total of 5×10^4 ADMSCs were seeded into each well of a six-well plate. At 80% to 90% confluence, ADMSCs were cultured in α-MEM that contained 10% FBS, 100 units/mL

penicillin, 0.292 mg/mL glutamine, 2 μmol/L insulin (Sigma-Aldrich, USA), 100 μg/mL streptomycin, 10 nmol/L dexamethasone (Sigma-Aldrich, USA), and 0.5 mmol/L isobutylmethylxanthine (Sigma-Aldrich, USA). The medium was changed every 2 days. After 14 days of conditioned culturing, cells were fixed with 4% paraformaldehyde and stained with an Oil Red O (Sigma-Aldrich, USA) solution for 20 min. The cells were observed under a phase-contrast inverted microscope after washing twice in PBS.

Osteogenic differentiation assays

A total of 5×10^4 ADMSCs were seeded into each well of the six-well plate. At 50% to 60% confluence, ADMSCs were cultured in α-MEM that contained 10% FBS, 100 units/mL penicillin, 0.292 mg/mL glutamine, 100 μg/mL streptomycin, 5 mmol/L L-glycerophosphate (Sigma-Aldrich, USA), 50 μg/mL ascorbic acid, and 10 nmol/L dexamethasone (Sigma-Aldrich, USA). The medium was changed every two days. After 21 days of conditioned culturing, the cells were fixed with 60% isopropanol for 1 min and 0.1% alizarin red solution (Sigma-Aldrich, USA) at room temperature for 3 min. The cells were observed under the phase-contrast inverted microscope after washing twice in PBS.

Preparation of stem cell-seeded scaffolds in vitro

ECM scaffolds were cut into 15 mm pieces on each side of the square and placed in the six-well plate with the removable bottom of the Transwell chamber used to press and prevent scaffold suspension. Scaffolds were covered with 200 μL of culture medium alone in the scaffold groups and with an equal volume of cell suspension that contained 5×10^5 ADMSCs in the ADMSC-scaffold group. After 4 h of incubation, 2 mL of culture medium was added to each well. The cells were incubated under standard culture medium with 50 μg/mL ascorbic acid for 3 days. ADMSC aggregate-ECM was tested with scanning electron microscopy (SEM; Hitachi S-4800, Japan) and confocal laser scanning microscopy (Olympus FV1000, Japan) and used for transplantation in animal models.

Effect of scaffold on growth factor secretion by ADMSCs

Real-time polymerase chain reaction analysis

Total RNA isolated from ADMSCs was used for quantitative polymerase chain reaction (q-PCR). RNA was collected using TRIzol reagent (Invitrogen Life Technology, USA) and reverse transcribed into cDNA according to the manufacturer's protocol. q-PCR was performed using SYBR green dye and a Light Cycler Instrument (Toyobo, Japan). The glyceraldehyde-3-phosphate dehydrogenase (GAPDH, Sangon Biotech, China) gene was analyzed and normalized for each cDNA sample. Gene expression was calculated using the comparative CT method. Primer sequences were as follows: transforming growth factor beta (TGF-β, Sangon Biotech, China): 5′-primer (5′-ATGTGTTCCTGCAGCACTGA-3′) and 3′-primer (5′-CGGACTGCTGGTGGTGTATT-3′); hepatocyte growth factor (HGF, Sangon Biotech, China): 5′-primer (5′-CAAACTTGTGCCAGTCCTGC-3′) and 3′-primer (5′-GTTGGCACATTGGTCTGCTG-3′); epidermal growth factor (EGF, Sangon Biotech, China): 5′-primer (5′-TGCCAACTGGGGGTGCACAG-3′) and 3′-primer (5′-CTGCCCGTGGCCAGCGTGGC-′); and GAPDH: 5′-primer (5′-CCTGCCGCCTGGAGAAAG-3′) and 3′-primer (5′-CCACCACCCTGTTGCTGTAG-3′).

Scanning electron microscopy

SEM was used to detect ADMSC aggregate-ECM. The combinations were washed twice with PBS and fixed with 3% glutaraldehyde for 1 day. After thoroughly washing with PBS twice for 10 min each, the samples were dehydrated by gradual change of ethanol concentrations (30%, 50%, 70%, 80%, 90%, 95%, and 100%) at 15 min intervals, sputter-coated with platinum, and moved under a scanning electron microscope (Hitachi S-4800, Japan) for observation.

Flow cytometry analysis

A total of 5×10^5 cells were seeded onto the ECM, cultured for 24 h in the 6-well plate, and collected as previously described. Digestive single cells were washed twice with PBS and resuspended in 67% cold alcohol for fixing at 4°C for 24 h. Finally, the cells were washed with PBS for 5 min and stained with 100 mg/mL propidium iodide (PI, Sigma-Aldrich, USA) at 4°C for 30 min. Elite ESP flow cytometry (Beckman Coulter, USA) was used for cell cycle analysis.

Full-thickness cutaneous wound models

Full-thickness cutaneous wound in ear auricle

A total of 36 three-month-old New Zealand white rabbits, regardless of gender, were selected. The rabbits were randomized into three treatment groups, namely, ADMSC aggregate-ECM, ECM, and control. Each rabbit was anesthetized through intravenous injection of pentobarbital. Thereafter, a 1.5 cm × 1.5 cm full-thickness skin in depth and perichondrium was sharply excised along the outline with a pair of scissors in the distal areas of each ear auricle. In the ECM and ADMSC aggregate-ECM groups, the grafts were removed from the PBS and placed into the dorsal wound, and two layers of Vaseline gauze were fixed on the grafts. In the control group, the defect area was only covered with two layers of Vaseline gauze.

Full-thickness cutaneous wound in auditory meatus

Twenty-seven New Zealand white rabbits as previously described were randomly allocated into the following three groups: ADMSC aggregate-ECM, ECM, and control. Near the root of the outer ear canal, outside skin, muscle, and cartilage were cut and stripped individually until the outer ear canal skin, and a 10-mm-diameter punch biopsy instrument was moderately forced onto the outer ear canal skin to circumcise the skin, thereby creating a 10-mm-diameter region. Subsequently, gelatin sponges were filled

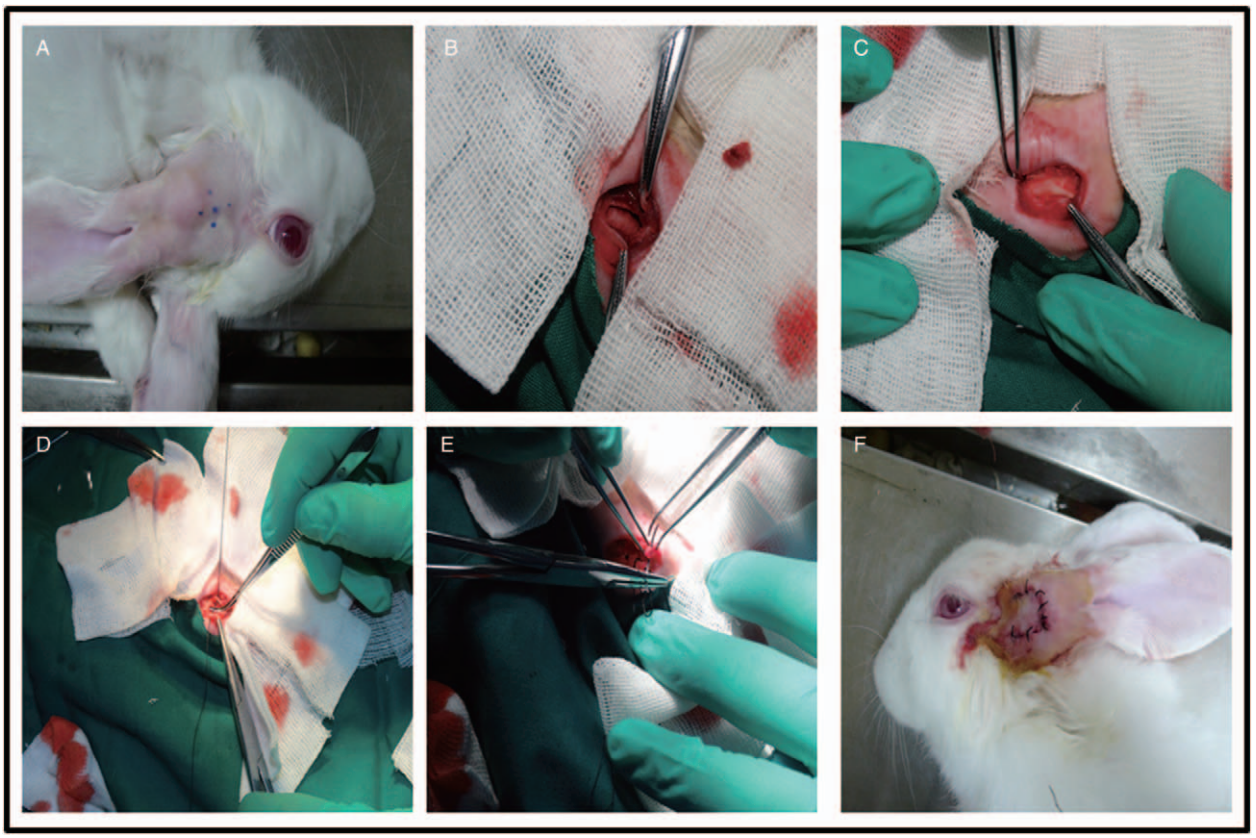

Figure 1: Schematics and photographic description of the experimental model used for the study. (A) The skin near the root of the outer ear canal is marked. (B) The outer skin, muscle, and cartilage are cut and stripped individually up to the outer ear canal's skin. A 10-mm-diameter punch biopsy instrument is moderately forced onto the outer ear canal skin to circumcise the skin to create a 10-mm-diameter region. (C) Gelatin sponges are filled in the outer ear canal to support the grafts that covered the defective area in the ECM and ADMSC aggregate-ECM groups. (D–F) The cartilage, muscle, and skin are sewn up. ADMSC: Adipose-derived mesenchymal stem cell; ECM: Extracellular matrix.

in the outer ear canal to support the grafts, which covered the defect area in the ECM and ADMSC aggregate-ECM groups. In the control group, the outer ear canal was only filled with gelatin sponges [Figure 1].

Western blotting

The total cellular proteins of the wound area skin samples after surgery at weeks 1 and 2 were immediately extracted with a homogenization buffer that contained phenylmethylsulfonyl fluoride, leupeptin, and other protease inhibitors on ice. Equal quantities of protein (20 μg) were separated by 12% sodium dodecyl sulfate-polyacrylamide gel and transferred onto polyvinylidene fluoride membranes using a Bio-Rad wet transfer unit. Next, the protein was incubated with HGF rabbit anti-human polyclonal antibody (LifeSpan BioSciences, USA), EGF rabbit anti-human polyclonal antibody (LifeSpan BioSciences, USA), bFGF polyclonal antibody (Abnova, China), TGF-beta1 antibody (Novus, USA), and VEGF rabbit anti-human polyclonal antibody (LifeSpan BioSciences, USA) at 4°C overnight. After incubation with secondary antibodies, the membrane was subjected to chemiluminescent detection on the next day. Actin was used to normalize the amount of loaded protein.

Histological analysis

Full-thickness biopsies of the wound-repair bed and surrounding tissue were obtained at 2, 4, and 7 weeks after operation of the in-ear auricle model and obtained at 4 weeks after operation of the outer ear canal model. The cells were fixed with 4% paraformaldehyde and routinely processed into 4-μm-thick paraffin-embedded sections. Then paraffin sections were stained with hematoxylin and eosin (H&E) staining and visualized in a bright field using a microscope (BX-51; Olympus, Japan). The scar elevation index was calculated as follows: (maximum thickness of scar skin–thickness of adjacent normal skin)/thickness of adjacent normal skin.

Wound healing analysis

To analyze wound healing, we imaged the wounds with appropriate distance calibration and standardization using a digital camera after surgery at 0, 2, 4, and 7 weeks in the in-ear auricle model and analyzed the photoprints using Image J image analysis software (National Institutes of Health). The percentage of wound closure was calculated as follows: (area of original wound–area of actual wound)/area of original wound × 100%.

Statistical analysis

Data were expressed as the mean ± standard deviation (SD). Statistical significance was determined using the Statistical Program for Social Science 23.0 for Windows. Comparisons of two and three groups were conducted by independent sample *t* test and one-way analysis of variance (ANOVA), respectively. A value of $P < 0.05$ denoted statistical significance.

Results

Characterization of ADMSCs

Rabbit ADMSCs of the fifth passage were cultured to adhere in Petri dishes with a long spindle shape and a radial arrangement through observation under the microscope. A positive result was observed for the mesenchymal stem cell markers CD90 and CD29, whereas a negative result was obtained for the monocyte marker CD14 and hematopoietic cell marker CD45 [Figure 2A]. Meanwhile, cells showed exponential growth, which reached a peak at 5 to 6 days [Figure 2B]. The abovementioned cells would differentiate into osteoblasts [Figure 2C] and adipocytes [Figure 2D] when cultured under appropriate differentiation condition. These results suggest that our ADMSCs maintained the common features of MSCs, which are coincident with those in previous studies.[17]

Characteristics of scaffolds and effects of scaffolds on proliferation of ADMSCs

SEM micrographs showed that the ECM scaffold possessed an imperforate bottom with uneven thickness, widely interconnected collagen bundle, and surface uplift of the lump [Figure 3A]. Hoechst33342/PI double staining showed that no cellular component was present in the ECM scaffold [Figure 3C]. This finding indicated that the cells were completely removed from the ECM. In comparison with the negative control, ADMSCs tightly adhered and actively migrated along the ECM surface to form cell sheets rapidly. SEM micrographs revealed that ADMSCs grew in a random arrangement and were overlapped [Figure 3B]. The close connection hindered a clear observation of single-cell morphology. This finding was confirmed by Hoechst 33342/PI double staining results, which showed massive blue and fractional red nuclei in the ECM [Figure 3D]. The percentage of ADMSCs that were seeded on the ECM was higher in the S phase and lower in the G1 phase than those in the control group [Figure 3E and 3F]. Thus, the ECM may stimulate ADMSCs to shift from G0G1 to the S phase.[18,19] The results of q-PCR indicated that the TGF-β, EGF, and HGF gene expression levels were increased in ADMSCs that were cultured on the ECM for 3 days compared with those in the control group

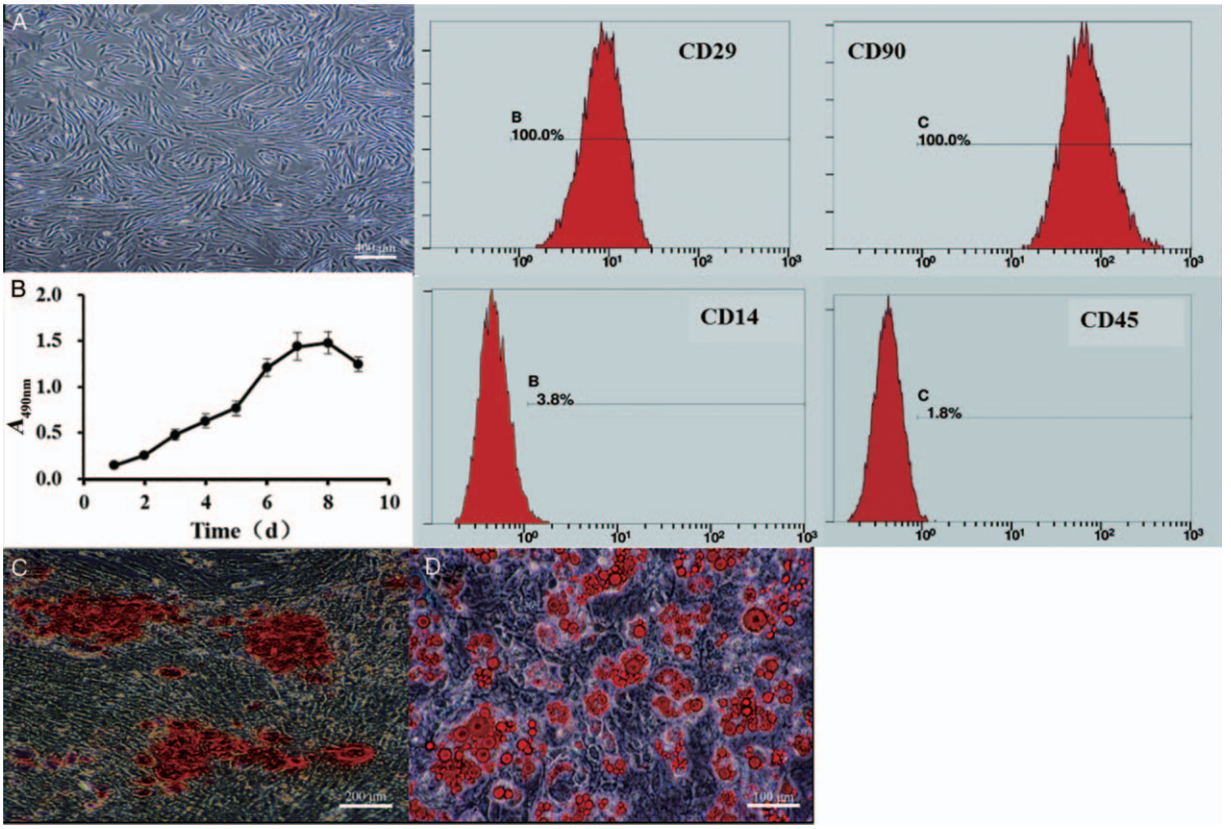

Figure 2: Characterization of rabbit ADMSCs. (A) Microscopic appearance of ADMSCs and flow cytometry analysis of ADMSCs. Representative diagrams are provided for CD29, CD90, CD14, and CD45 expressions. Scale bar represents 400 μm. (B) Assessment of cellular viability via the MTT assay at 1 to 9 days. (C) Alizarin red staining of ADMSCs that are cultured in estrogenic medium. Scale bar represents 200 μm. (D) Oil Red O staining of ADMSCs that are cultured in radiogenic medium. Scale bar represents 100 μm. ADMSC: Adipose-derived mesenchymal stem cell; MTT: 3-(4, 5-dimethylthiazol-2-yl)-2, 5-diphenyltetrazolium bromide.

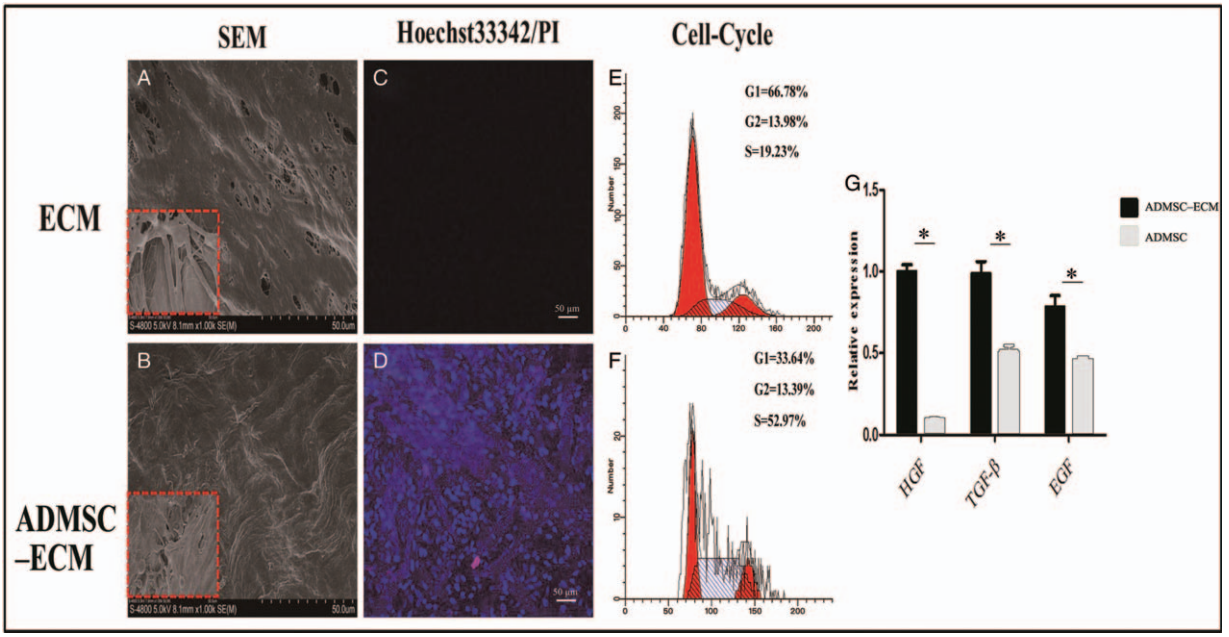

Figure 3: Effects of the scaffolds on the morphology, apoptosis, proliferation, and secretion of ADMSCs. (A) SEM photographs of the ECM and (B) ADMSCs cultured *in vitro* for 3 days on the ECM. Scale bars represent 50 μm. (C) Hoechst 33342/PI staining of the ECM and (D) ADMSCs cultured on ECM. Scale bars represent 50 μm. (E) Flow cytometry analysis of the cell cycle distributions of ADMSCs and (F) ADMSCs cultured on ECM. (G) Real-time q-PCR results for the mRNA expression of HGF, TGF-β, and EGF by ADMSCs cultured on ECM. Mean ± SD of $n = 3$ independent determinations are shown. $^{*}P < 0.05$. ADMSC: Adipose-derived mesenchymal stem cell; ECM: Extracellular matrix; EGF: Epidermal growth factor; HGF: Hepatocyte growth factor; q-PCR: Quantitative polymerase chain reaction; SD: Standard deviation; SEM: Scanning electron microscopy; TGF-β: Transforming growth factor-β.

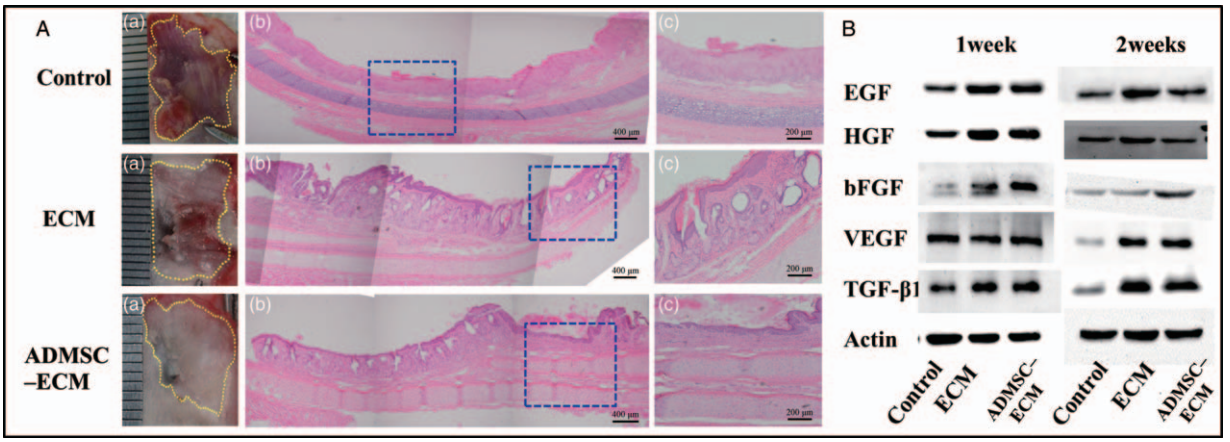

Figure 4: Wound repair and expression levels of growth factors in the auditory meatus at 4 weeks after surgery. (A) (a) General observations and H&E staining of the wound regions are recorded on week 4 after the creation of excisional wounds in the auditory meatus. (b) Low magnification. Scale bars represent 400 μm. (c) Higher magnification. Scale bars represent 200 μm. (B) Western blotting reveal the expression levels of EGF, HGF, bFGF, VEGF, and TGF-β1 at weeks 1 and 2. ADMSC: Adipose-derived mesenchymal stem cell; bFGF: Basic fibroblast growth factor; ECM: Extracellular matrix; EGF: Epidermal growth factor; HGF: Hepatocyte growth factor; TGF-β1: Transforming growth factor-β1; VEGF: Vascular endothelial growth factor.

[Figure 3G]. These results indicated that the scaffold could positively support cell proliferation.

Repairing rabbit skin defects of auditory meatus

Image J image analysis software was used to analyze the photographs of the epithelialization of the wound bed in the auditory meatus at 4 weeks after surgery. Skin formed, which was nearly consistent with the surrounding tissue in the ADMSC aggregate-ECM group. However, skin partially formed in the two other groups [Figure 4A(a)]. H&E staining showed that a partial region of tissue was formed in the ADMSC aggregate-ECM and ECM groups. However, epidermal formation was not found in the control group [Figure 4A(b)]. In addition, the ADMSC aggregate-ECM group had a larger range of normal skin-like structure than that of the ECM group [Figure 4A(c)]. Western blot results indicated that a correlation exists between particular growth factor levels and the wound healing process. At weeks 1 and 2, the levels of bFGF, EGF, HGF, VEGF, and TGF-β1 in the ADMSC aggregate-ECM and ECM groups were significantly higher than those in the control group [Figure 4B].

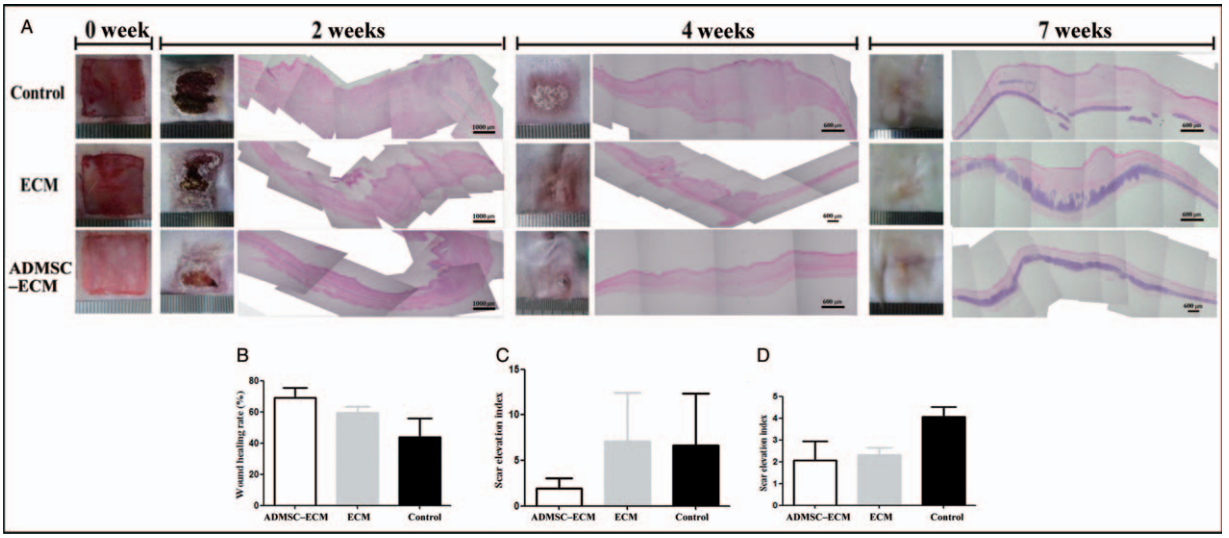

Figure 5: Wound repair in the ear auricle at 0, 2, 4, and 7 weeks after surgery. (A) General observations and hematoxylin and eosin staining of the wound regions are recorded on weeks 0, 2, 4, and 7 after the creation of excisional wounds in the ear auricle. (B) The percentage of the wound area is calculated using photographs of the wound at week 2. (C–D) Analysis of the scar elevation index on postoperative weeks 4 and 7. Mean ± standard deviation of $n = 6$ independent determinations are shown, Scale bars represent 1000 μm and 600 μm.

Repairing rabbit skin defects of ear auricle

Image J image analysis software was used to analyze the photographs of the epithelialization of the wound bed in the ear auricle at 0, 2, 4, and 7 weeks after surgery. At 2 weeks, the wound healing rates in the ADMSC aggregate-ECM (69.02 ± 6.36%) and ECM (59.32 ± 4.10%) groups were higher than that in the control group (43.74 ± 12.15%) ($F = 14.290$, $P < 0.001$; $P = 0.005$, $P < 0.001$). However, no significant difference was found between the wound healing rates of the ADMSC aggregate-ECM and ECM groups ($P = 0.060$) [Figure 5B]. In addition, inflammatory reaction was strongest in the control group [Figure 5A]. At 4 weeks, the wounds in all of the groups were completely healed [Figure 5A]. However, no significant difference in the scar elevation index was found in the ADMSC aggregate-ECM (1.95 ± 1.12), ECM (7.14 ± 5.26), and control (6.68 ± 5.68) groups ($F = 2.425$, $P = 0.122$; Figure 5C). At 7 weeks, in comparison with control (4.06 ± 0.45), the scar elevation index in the ADMSC aggregate-ECM (2.08 ± 0.87) and ECM (2.31 ± 0.33) groups were lower ($F = 19.724$, $P < 0.001$; $P < 0.001$, $P < 0.001$; Figure 5D). The analysis showed that the scar elevation index of the ADMSC aggregate-ECM group reached the lowest rate 4 weeks in advance [Figure 5C and 5D].

Discussion

We attempted to achieve a rapid post-operative regeneration of temporal bone mastoid cavity skin on the exposed bone surface to prevent postoperative complications. Our findings demonstrated that ADMSC aggregate-ECM and ECM exerted good effectiveness in rapid skin regeneration when transplanted into the ear auricle and external auditory canal of rabbits. Of the two groups, ADMSC aggregate-ECM displayed better performance.

Previously, autologous-cultured keratinocyte layers,[7] autologous epithelial layers from the buccal epithelium,[5] allogeneic ear keratinocyte sheets,[6] mucosal cell sheet grown on collagen gel populated with fibroblasts,[20,21] and nasal mucosal epithelial cell sheets[22] have been fabricated to promote the regeneration of external auditory canal and middle ear skin or mucosa after cutaneous transplantation. Long-term epithelial repair that utilizes these grafts in the ears presents continuous and resistant otorrhea without evidence of the recurrence of granulation tissue after a follow-up period that ranges from 10 to 18 months.[6] However, upon actual clinical application of this method to humans, numerous problems and ethical issues must be resolved. In these methods, normal epidermal cells have to be harvested from the ear skin, buccal epithelium, or nasal mucosa as a potential cell source. However, obtaining a sufficient amount of suitable normal tissue for culture is difficult due to several reasons, such as severe lesions in the middle ear cavity of cholesteatoma and change in surgical methods. In addition, the approach leads to the decomposition of normal nasal and buccal mucosal tissue, thereby resulting in nasal and oral discomfort. These approaches are thus equal to addressing one problem while causing another, which raises ethical issues. Therefore, ADMSC aggregate-ECM and ECM offer new approaches that can be developed to promote skin regeneration after surgery in consideration of the clinical application to actual humans in the future. These methods also exhibit an advantage of ECM, which provides a supportive medium or adequate nutrition for ADMSC survival. Conversely, we are not concerned that the simple cell sheet grafts may lead to worse contractions than those that occur with conventional split-thickness grafts.

The ECM scaffolds we used were provided by the Center for Tissue Engineering, School of Stomatology, Fourth

Military Medical University. These scaffolds were created from porcine peritoneum to remove resident cells by mechanical curettage and hypertonic saline solution. We evaluated the influences of these ECM scaffolds on the adherence, proliferation, and ability of the secreting growth factor of ADMSCs *in vitro*. ADMSCs in the ECM adhered well and formed cell sheets after seeding for 4 h and 3 days. Previous studies have shown that epidermal cells, which are separated, proliferate until cell sheets are formed for the application of a minimum of 1 month. Our results suggested that ADMSCs could reduce the application and waiting time of patients. ADMSCs cultured in the ECM proliferated faster than those that were directly cultured in six-well plates. Meanwhile, ECM significantly inhibited cell apoptosis to enhance the survival of ADMSCs. Our results suggested that ECM could function as a suitable scaffold, which could be designed and manufactured to suit the seeding cells. ADMSCs that were seeded in the ECM secreted higher levels of TGF-β, HGF, and EGF than those seeded directly in six-well plates. However, when the ECM was cultured under the same culture conditions, none of the RNAs were isolated. These results indicated that the ECM scaffold could supply a better living 3D environment for cells and induce cells to secrete a larger number of factors, which are vital for tissue repair and remodeling. These results are consistent with those of previous studies.[23] The ECM did not degrade in TRIzol; thus, the RNAs of growth factors were undetected. Overall, the structurally and functionally different molecules in the ECM scaffolds may support the proliferation and secretion of growth factors by the seeded cells.[15,16]

In this study, skin regeneration occurred at higher rates in the ADMSC aggregate-ECM and ECM groups compared with the control group at 2 weeks. Transplantation in early histological studies showed positive epithelial engraftment on the transplanted site, which indicated that ADMSC aggregate-ECM and ECM therapy regulate inflammation, thereby forming a low inflammatory, partial, and wound healing microenvironment.[24-27] At 4 weeks, the ADMSC aggregate-ECM group reached the lowest rate in advance in relation to the scar elevation index and had the largest range of normal skin-like structure at 4 weeks. Our results may be related to the wound repair-promoting effects of functionality, which is not only due to the grafting process but also attributed to the stimulation of wound repair mechanisms by ADMSCs. Although several studies have shown that the decellularization process may be unable to eliminate all cellular elements, which could potentially express minor antigens and subsequently induce chronic rejection,[28-30] our ECM did not exhibit evident inflammatory infiltrates, which indicated the excellent biocompatibility of the scaffolds. Meanwhile, histological studies have shown that by covering the cartilage surface with the transplanted ADMSC aggregate-ECM and ECM, cartilage hyperplasia was enhanced.

The release of growth factors by ADMSCs might induce the migration and proliferation of resident epithelial cells that are present at the wound edges. This mechanism is the main theory for mesenchymal stem cells that promote wound healing. In this study, ECM transplants also secreted larger amounts of EGF, HGF, TGF-β1, bFGF, and VEGF than the control at weeks 1 and 2. These data suggest that ECM may support tissue proliferation and secretion of growth factors through structurally and functionally different molecules during self-degradation.[23] TGF-β is a chemotactic for fibroblasts, keratinocytes, and inflammatory cells.[31] Furthermore, TGF-β suppresses inflammatory reactions, which leads to transition to the proliferative phase[32] and promotes ECM deposition.[6] EGF acts via desmosomes and hemidesmosomes to re-establish cell adhesion.[31] VEGF is the most effective and specific growth factor that regulates angiogenesis.[33] bFGF is a potent mitogen and chemoattractant for endothelial cells, fibroblasts, and keratinocytes. The factor stimulates the metabolism and growth of the ECM, as well as the movement of mesodermally derived cells.[34] In addition, bFGF accelerates wound healing and improves the quality of scars by regulating the balance of collagen synthesis and degradation.[33] Overall, bFGF, TGF-β, EGF, HGF, and VEGF are powerful inducers of proliferation and migration of epithelial cells, as well as promoters of neoangiogenesis.[31-35]. Western blot results also suggest that selecting suitable scaffolds can promote the secretion of factors during the reduction of inflammation *in vivo*. A previous study has shown that similar results prevent the need for transfection and fulfil the vascularization requirement.[15,36]

One limitation of our study is that although we confirmed that ADMSC aggregate-ECM and ECM could accelerate wound closure with increased re-epithelialization and inhibit scar formation in a person's external ear canal, the temporal bone structure is crucial for skin gas exchange because the temporal bone structure is subjected to the partial pressure gradient between the ear cavity and skin capillaries via the skin.[37,38] The epithelium of the ear canal presents a unique migration ability.[39-41] Migration occurs because of the unique proliferative capacity of the epithelium and F-actin cytoskeleton, which is a protein with contractile properties, in the basal layers of the ear canal epithelium.[42] Therefore, finding the appropriate model to observe the effect of ADMSC aggregate-ECM is difficult.

In conclusion, we conclude that ADMSC aggregate-ECM exhibits a potential for use as a graft material for wound healing of the auricle and auditory meatus. Our results also suggest that simple ECM may be convenient and meaningful for use in clinical practice in the absence of suitable conditions for cell culture. This approach will provide a meaningful experimental basis for mastoid epithelium repair in subsequent clinical trials.

Funding

This study was supported by a grant from the National Natural Science Foundation of China (No. 81170904).

Conflicts of interest

None.

References

1. Premachandra DJ, Woodward BM, Milton CM, Serqeant RJ, Fabre JW. Treatent of postoperative otorrhoea by grafting of mastoid cavities with cultured autologous epidermal cells. Lancet 1990;335:365–367. doi: 10.1016/0140-6736(90)90204-I.
2. Renton JP, Wetmore SJ. Split-thickness skin grafting in postmastoidectomy revision and in lateral temporal bone resection. Otolaryngol Head Neck Surg 2006;135:387–391. doi: 10.1016/j.otohns.2005.10.065.
3. Lee DH, Jun BC, Jung SH, Song CE. Deep temporal fascial-periosteal flap for canal wall down mastoidectomy. Laryngoscope 2006;116:2229–2231. doi: 10.1097/01.mlg.0000245976.01691.c6.
4. Roche P, Coolahan I, Glynn F, Mc Conn WR. Autologous bone pate in middle ear and mastoid reconstruction. Rev Laryngol Otol Rhinol (Bord) 2011;132:193–196.
5. Minoda R, Hayashida M, Masuda M, Yumoto E. Preliminary experience with beta-tricalcium phosphate for use in mastoid cavity obliteration after mastoidectomy. Otol Neurotol 2007;28:1018–1021. doi: 10.1097/MAO.0b013e3181557b7c.
6. Premachandra DJ, Woodward BM, Milton CM, Serqeant RJ, Fabre JW. Treatment of chronic mastoiditis by grafting of mastoid cavities with autologous epithelial layers generated by in vitro culture of buccal epithelium. J Laryngol Otol 1991;105:413–416. doi: 10.1017/S0022215100116172.
7. Somers T, Verbeken G, Vanhalle S, Delaey B, Duinslaeger L, Govaerts P, *et al*. Treatment of chronic postoperative otorrhea with cultured keratinocyte sheets. Ann Otol Rhinol Laryngol 1997;106:15–21. doi: 10.1177/000348949710600103.
8. Somers T, Duinslaeger L, Delaey B, Verbeken G, Van Halle S, Boedts D, *et al*. Stimulation of epithelial healing in chronic postoperative otorrhea using lyophilized cultured keratinocyte lysates. Am J Otol 1997;18:702–706.
9. Kanazawa YJ, Shojaku H, Okabe M, Fujisaka M, Takakura H, Tachino H, *et al*. Application of hyperdry amniotic membrane patches without fibrin glue over the bony surface of mastoid cavities in canal wall down tympanoplasty. Acta Otolaryngol 2012;132:1282–1287. doi: 10.3109/00016489.2012.701329.
10. Egaña JT, Fierro FA, Krüger S, Bornhäuser M, Huss R, Lavandero S, *et al*. Use of human mesenchymal cells to improve vascularization in a mouse model for scaffold-based dermal regeneration. Tissue Eng Part A 2009;15:1191–1200. doi: 10.1089/ten.tea.2008.0097.
11. Nakagami H, Maeda K, Morishita R, Iguchi S, Nishikawa T, Takami Y, *et al*. Novel autologous cell therapy in ischemic limb disease through growth factor secretion by cultured adipose tissue-derived stromal cells. Arterioscler Thromb Vasc Biol 2005;25:2542–2547. doi: 10.1161/01.ATV.0000190701.92007.6d.
12. Domingues JA, Cherutti G, Motta AC, Hausen MA, Oliveira RT, Silva-Zacarin EC, *et al*. Bilaminar device of Poly(Lactic-co-Glycolic Acid)/Collagen cultured with adipose-derived stem cells for dermal regeneration. Artif Organs 2016;40:938–949. doi: 10.1111/aor.12671.
13. Lindroos B, Suuronen R, Miettinen S. The potential of adipose stem cells in regenerative medicine. Stem Cell Rev 2011;7:269–291. doi: 10.1007/s12015-010-9193-7.
14. McIntosh KR, Lopez MJ, Borneman JN, Spencer ND, Anderson PA, Gimble JM. Immunogenicity of allogeneic adipose-derived stem cells in a rat spinal fusion model. Tissue Eng Part A 2009;15:2677–2686. doi: 10.1089/ten.TEA.2008.0566.
15. Liu S, Zhang H, Zhang X, Lu W, Huang X, Xie H, *et al*. Synergistic angiogenesis promoting effects of extracellular matrix scaffolds and adipose-derived stem cells during wound repair. Tissue Eng Part A 2011;17:725–739. doi: 10.1089/ten.TEA.2010.0331.
16. Badylak SF, Freytes DO, Gilbert TW. Extracellular matrix as a biological scaffold material: structure and function. Acta Biomater 2009;5:1–13. doi: 10.1016/j.actbio.2008.09.013.
17. Moore MC, Pandolfi V, McFetridge PS. Novel human-derived extracellular matrix induces in vitro and in vivo vascularization and inhibits fibrosis. Biomaterials 2015;49:37–46. doi: 10.1016/j.biomaterials.2015.01.022.
18. Semyari H, Rajipour M, Sabetkish S, Sabetkish N, Abbas FM, Kajbafzadeh AM. Evaluating the bone regeneration in calvarial defect using osteoblasts differentiated from adipose-derived mesenchymal stem cells on three different scaffolds: an animal study. Cell Tissue Bank 2015;17:69–83. doi: 10.1007/s10561-015-9518-5.
19. Zhou YL, Yan Z, Zhang H, Lu W, Liu S, Huang X, *et al*. Expansion and delivery of adipose-derived mesenchymal stem cells on three microcarriers for soft tissue regeneration. Tissue eng Part A 2011;17:2981–2997. doi: 10.1089/ten.tea.2010.0707.
20. Yaguchi Y, Wada K, Uchimizu H, Tanaka Y, Kojima H, Moriyama H. Middle ear mucosa regeneration by grafting of artificial mucosa. Acta Otolaryngol 2007;127:1038–1044. doi: 10.1080/00016480701200285.
21. Wada K, Tanaka Y, Kojima H, Inamatsu M, Yoshizato K, Moriyama H. In vitro reconstruction of a three-dimensional middle ear mucosal organ and its in vivo transplantation. Acta Otolaryngol 2006;126:801–810. doi: 10.1080/00016480500507385.
22. Yamamoto K, Hama T, Yamato M, Uchimizu H, Sugiyama H, Takagi R, *et al*. The effect of transplantation of nasal mucosal epithelial cell sheets after middle ear surgery in a rabbit model. Biomaterials 2015;42:87–93. doi: 10.1016/j.biomaterials.2014.11.037.
23. Badylak SF. The extracellular matrix as a biologic scaffold material. Biomaterials 2007;28:3587–3593. doi: 10.1016/j.biomaterials.2007.04.043.
24. Choi H, Lee RH, Bazhanov N, Oh JY, Prockop DJ. Anti-inflammatory protein TSG-6 secreted by activated MSCs attenuates zymosan-induced mouse peritonitis by decreasing TLR2/NF-kappaB signaling in resident macrophages. Blood 2011;118:330–338. doi: 10.1182/blood-2010-12-327353.
25. Qi Y, Jiang D, Sindrilaru A, Stegemann A, Schatz S, Treiber N, *et al*. TSG-6 released from intradermallyb injected mesenchymal stem cells accelerates wound healing and reduces tissue fibrosis in murine full-thickness skin wounds. J Invest Dermatol 2014;134:526–537. doi: 10.1038/jid.2013.328.
26. Liu SY, Jiang L, Li H, Shi H, Luo H, Zhang Y, *et al*. Mesenchymal stem cells prevent hypertrophic scar formation via inflammatory regulation when undergoing apoptosis. J Invest Dermatol 2014;134:2648–2657. doi: 10.1038/jid.2014.169.
27. Jungebluth P, Go T, Asnaghi A, Bellini S, Martorell J, Calore C, *et al*. Structural and morphologic evaluation of a novel detergent-enzymatic tissueengineered tracheal tubular matrix. J Thorac Cardiovasc Surg 2009;138:586–593. doi: 10.1016/j.jtcvs.2008.09.085.
28. Macchiarini P, Jungebluth P, Go T, Asnaghi MA, Rees LE, Cogan TA, *et al*. Clinical transplantation of a tissue-engineered airway. Lancet 2008;372:2023–2030. doi: 10.1016/S0140-6736(08)61598-6.
29. Conconi MT, De Coppi P, Di Liddo R, Vigolo S, Zanon GF, Parnigotto PP, *et al*. Tracheal matrices, obtained by a detergent-enzymatic method, support in vitro the adhesion of chondrocytes and tracheal epithelial cells. Transpl Int 2005;18:727–734. doi: 10.1111/j.1432-2277.2005.00082.x.
30. Zang M, Zhang Q, Chang EI, Mathur AB, Yu P. Decellularized tracheal matrix scaffold for tracheal tissue engineering: in vivo host response. Plast Reconstr Surg 2013;132:549e–559e. doi: 10.1097/PRS.0b013e3182a013fc.
31. Hantash BM, Zhao L, Knowles JA, Lorenz HP. Adult and fetal wound healing. Front Biosci 2008;13:51–61. doi: 10.2741/2559.
32. Dobaczewski M, Gonzalez-Quesada C, Frangogiannis NG. The extracellular matrix as a modulator of the inflammatory and reparative response following myocardial infarction. J Mol Cell Cardiol 2010;48:504–511. doi: 10.1016/j.yjmcc.2009.07.015.
33. Seo E, Lim JS, Jun JB, Choi W, Hong IS, Jun HS. Exendin-4 in combination with adipose-derived stem cells promotes angiogenesis and improves diabetic wound healing. J Transl Med 2017;15:35. doi: 10.1186/s12967-017-1145-4.
34. Shi HX, Lin C, Lin BB, Wang ZG, Zhang HY, Wu FZ, *et al*. The anti-scar effects of basic fibroblast growth factor on the wound repair in vitro and in vivo. PLoS One 2013;8:e59966. doi: 10.1371/journal.pone.0059966.
35. Peura M, Bizik J, Salmenperä P, Noro A, Korhonen M, Pätilä T, *et al*. Bone marrow mesenchymal stem cells undergo nemosis and induce keratinocyte wound healing utilizing the HGF/c-Met/PI3K pathway. Wound Repair Regen 2009;17:569–577. doi: 10.1111/j.1524-475X.2009.00507.x.
36. Bleiziffer O, Eriksson E, Yao F, Horch RE, Kneser U. Gene transfer strategies in tissue engineering. J Cell Mol Med 2007;11:206–223. doi: 10.1111/j.1582-4934.2007.00027.x.
37. Uchimizu H, Utahashi H, Hamada Y, Aoki K. Middle ear total pressure measurement as a useful parameter for outcome prediction in pediatric otitis media with effusion. Int J Pediatr Otorhinolaryngol 2005;69:1659–1665. doi: 10.1016/j.ijporl.2005.03.048.
38. Luntz M, Levi D, Sadé J, Herman H. Relationship between the gas composition of the middle ear and the venous blood at steady state. Laryngoscope 1995;105 (5 Pt 1):510–512. doi: 10.1288/00005537-199505000-00012.

39. Alberti PW. Epithelial migration on the tympanic membrane. J Laryngol Otol 1964;78:808–830.
40. Litton WB. Epidermal migration in the ear: the location and characteristics of the generation center revealed by utilizing a radioactive desoxyribose nucleic acid precursor. Acta Otolaryngol 1964;suppl 240:5.
41. Boedts D, Kuijpers W. Epithelial migration on the tympanic membrane. Acta Otolaryngol 1978;85:248–252.
42. Bonding P, Charabi S. Epithelial migration in mastoid cavities. Clin Otolaryngol Allied Sci 1994;19:306–309. doi: 10.1111/j.1365-2273.1994.tb01236.x.

How to cite this article: Zhang WJ, Ming LG, Sun JJ. Epithelial defect repair in the auricle and auditory meatus by grafting with cultured adipose-derived mesenchymal stem cell aggregate-extracellular matrix. Chin Med J 2019;132:680–689. doi: 10.1097/CM9.0000000000000125